PERIODICA POLYTECHNICA SER. MECH. ENG. VOL. 39, NOS. 3-4, PP. 167-187 (1995)

HIGH PRESSURE TANK FOR NATURAL GAS OPERATED VEHICLES[1]

László VARGA, András NAGY and Attila KOVÁCS

Institute for Machine Design
Technical University of Budapest
1111 Budapest, Hungary, Müegyetem rkp. 3.
Fax.:(36)-463-3510, Email.:kovacsa@inflab.bme.hu

Received: Febr. 3, 1995

Abstract

Compressed natural gas storage tank suitable for gas operated vehicles can be advantageously made of thin walled aluminium linear overwinded with glass/epoxy reinforcement. These materials combined show a perfect coacting of liner and composite shell and further on the high tensile strength of glass-fibre reinforced epoxy layers can be totally utilized. The advantages of the chosen construction can only be maximized in case of composite shell with optimal wall thickness and optimal prestressing of the tank. So the design task is to optimize the construction which can be done according to this paper. The reliability of the proposed design method together with advantages of the chosen structural solution are proved by the design, the manufacture, and testing of a prototype tank.

Keywords: aluminium liner, reinforced plastic, composite shell, hybrid structure, CNG tank, pressure, optimal stiffening, optimal prestressing.

1. Introduction

Among the present known fuels natural gas is one of the cheapest, the most environment friendly and provides the highest safety during operation. The most important part of the natural gas driven vehicles is the compressed natural gas storage tank (hereafter abbreviated as CNG tank). The safe operation requires the high-pressure tank to be able to withstands the multiple of filling pressure at static load and the multiple of the expected fatigue load cycles resulting from recharging without leakage or cracking. Furthermore the tank should keep pressure tightness in case of accidents, too. The tank fulfilling all the above requirements and at the same time meeting the requirement of mass production at a competitive price and having a small mass can be successful in the market. There are several CNG tanks avail-

[1]This paper resents the essence of the most important results achieved in a project realized as a common venture of TNO Plastics and Rubber Research Institute (Netherlands), CISE Technology Innovative (Italy), ANTE Materials Technology Union (Hungary) and Technical University of Budapest Institute for Machine Design (Hungary) and it was sponsored by the European Community.

able at present in the market manufactured from different engineering materials using different design. These tanks satisfy more or less the above mentioned requirements. The tank being discussed in this paper will increase the number of competitive products. In this paper the main characteristics of the new design together with the specific design methodology, manufacturing and testing of it will be described. It can be regarded as a hybrid structure where the aluminium alloy (AlMgSi1) liner mainly provides the gas-pressure tightness and corrosion resistance while the different angle filament wound glass-fibre reinforced epoxy outer shell withstand the load caused by the high internal pressure. This material mating is favourable because the aluminium is able to withstand the high strains so on one hand it guarantees a perfect coacting of liner and composite shell and on the other hand makes total utilization of the high tensile strength of the glass-fibre reinforced epoxy layers. The full value of the above advantages can only be realized provided the proper shape, tank stiffness and optimal prestressing of the tank used simultaneously. It is well-known that the minimum specific mass is obtained with a spherical shaped tank. CNG tanks have usually cylindrical shape with hemispherical heads to give better utilization of space and simpler manufacturing. The ratio of the length to diameter (l/d) is usually determined by the required useful volume and the space given, though the specific mass can be reduced by increasing this ratio [1]. All the further important parameters, among them the shape and structure of cross-sections required, the optimal values of stiffness and prestressing of the tank can only be calculated by detailed analysis and synthesis of the structure. The following sections deal with these questions by considering first the stress-state analysis of the structure, then calculating the optimal stiffness and prestressing. Finally the design, the manufacture and the test of the new construction is summarized.

2. Stress Analysis of a Hybrid Structure

In order to determine the stress-strain state of the investigated hybrid structure first of all models should be created. These models are the material model, the structural model and the load model. After creating the above models it should also be worked out the calculation model making possible to determine the stress-strain state. The composite shell consisting of different wound angle glass-fibre reinforced epoxy layers has been assumed to be linearly elastic following the rule of mixtures law for stiffness. The modulus of elasticities (E_{xi}, E_{yi}) and Poissons ratios (ν_{xyi}, ν_{yxi}) of the different layers (see *Fig. 1*) can be calculated in knowledge of the volume ratios and the elastic modulus of the glass fibers and the epoxy matrix.

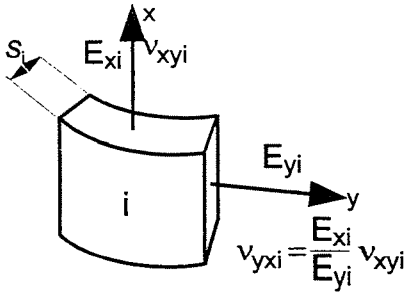

Fig. 1. Elastic properties of layers

According to the above assumptions the stress-strain relationship of the composite shell can be calculated from *Eq.* (1) where the different parameters come from *Eq.* $(2.a-c)$ [2].

$$\varepsilon_i = S_i \sigma_i \,, \tag{1}$$

$$\sigma_i = \begin{bmatrix} \sigma_{xi} \\ \sigma_{yi} \\ \sigma_{xyi} \end{bmatrix}, \quad \varepsilon_i = \begin{bmatrix} \varepsilon_{xi} \\ \varepsilon_{yi} \\ \varepsilon_{xyi} \end{bmatrix}, \quad S_i = \begin{bmatrix} \frac{1}{E_{xi}} & -\frac{\nu_{yxi}}{E_{xi}} & 0 \\ -\frac{\nu_{xyi}}{E_{yi}} & \frac{1}{E_{yi}} & 0 \\ 0 & 0 & \frac{1}{E_{xy}} \end{bmatrix}. \quad (2.\ a-c)$$

The stress-strain curve for the aluminium liner can be seen in *Fig. 2*. As the *Fig. 2* shows the liner material is homogeneous and isotropic. At the beginning it is ideally elastic, later it becomes plastic-strain hardening which can be linearized by ranges [3]. The above curve linearized in the range j according to the *Eq.* (1) can also be used where $E_{x1} = E_{y1} = E_1^j$ and $\nu_{xy1} = \nu_{yx1} = \nu_1^j \cong \nu_1$.

Regarding the model the major load is the internal pressure including its static and the varying parts. According to international recommendations [4, 5] the characteristic values and their relations are: the filling pressure ($p_f = 20$ MPa), the test pressure p_t ($p_t^*/p_f = 1.5$), the burst pressure p_b ($p_b/p_f = 2.35$) and the pressure p_F causing fatigue failure ($p_F/p_f = 0.125 \div 1.25$). Modelizing the engineering materials and acting loads, the stress-strain state of the structure can be predicted in advance using the finite elements method (FEM). These investigations are time consuming and require highly complicated labour input and should be repeated many times. Therefore, to avoid these problems a simplified method was developed. This method is more suitable for quick calculation of the stress-strain state at critical cross-sections in the cylindrical part of the tanks than the finite elements method. The results obtained can also be easily

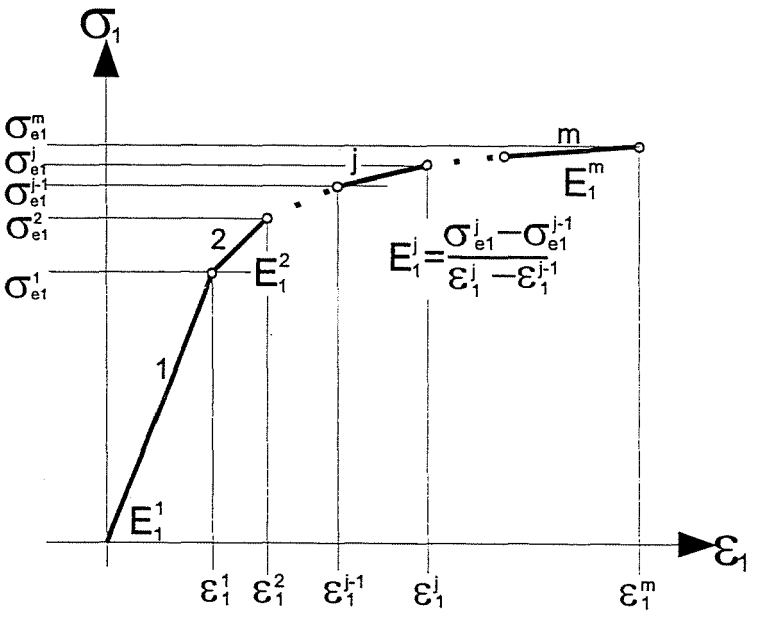

Fig. 2. Linearized stress-strain curve of the liner

evaluated to give conclusions concerning the optimized dimensions. The classical method gives directly the stresses caused by internal pressure both the longitudinal σ_{xi} and circumferential σ_{yi} directions in each layer of the composite shell (see *Fig. 3*).

In accordance with the equilibrium and strain conditions, *Eq.* (3) gives the relationship between loads and stress state of the cylindrical part which can also be written as *Eq.* (4).

The G_i matrices in *Eq.* (3) mean the geometric relationship among the different layers while p represents the pressure acting on the cylindrical part of the tank as shown in *Eq.* (5).

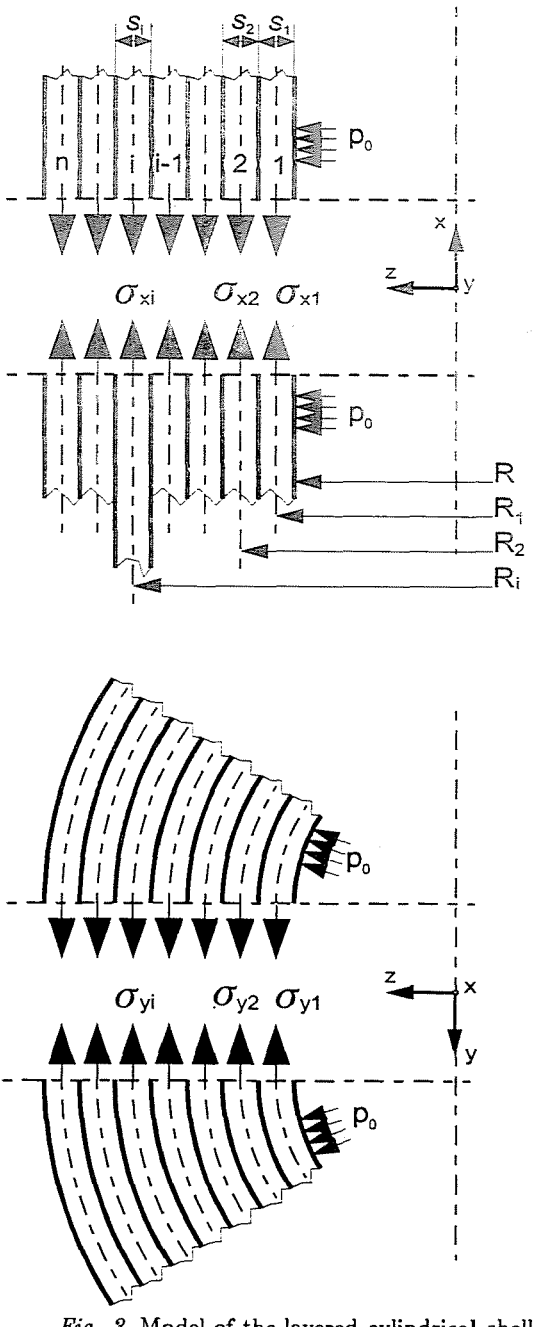

Fig. 3. Model of the layered cylindrical shell

$$\begin{bmatrix} S_1 & -S_2 & 0 & \cdot & \cdot & \cdot & \cdot & \cdot \\ 0 & S_2 & -S_3 & 0 & \cdot & \cdot & \cdot & \cdot \\ \cdot & 0 & S_3 & -S_4 & 0 & \cdot & \cdot & \cdot \\ \cdot & \cdot & 0 & \cdot & \ddots & \cdot & \cdot & \cdot \\ \cdot & \cdot & \cdot & \cdot & \cdot & \cdot & 0 & \cdot \\ \cdot & \cdot & \cdot & \cdot & 0 & S_{n-2} & S_{n-1} & 0 \\ \cdot & \cdot & \cdot & \cdot & \cdot & 0 & S_{n-1} & -S_n \\ G_1 & G_2 & \cdot & \cdot & \ldots & \cdot & G_{n-1} & G_n \end{bmatrix} \times \begin{bmatrix} \sigma_1 \\ \sigma_2 \\ \cdot \\ \vdots \\ \cdot \\ \cdot \\ \cdot \\ \sigma_n \end{bmatrix} = \begin{bmatrix} 0 \\ 0 \\ \cdot \\ \vdots \\ \cdot \\ \cdot \\ 0 \\ p \end{bmatrix}, \tag{3}$$

$$K\sigma = q\,, \tag{4}$$

$$G_i = \begin{bmatrix} \frac{2R_i s_i}{R^2} & 0 & 0 \\ 0 & \frac{s_i}{R} & 0 \\ 0 & 0 & 0 \end{bmatrix}, \quad p = \begin{bmatrix} p \\ p \\ 0 \end{bmatrix}. \tag{5}$$

First the stress-state of the cylindrical part generated by unit internal pressure can be calculated using *Eq.* (6)

$$\sigma^{*j} = (K^j)^{-1} q\Big|_{p=1}\,. \tag{6}$$

The equivalent stress in the aluminium liner can be calculated from *Eq.* (7)

$$\sigma_{e1}^{*j} = \sqrt{(\sigma_{x1}^{*j})^2 + (\sigma_{y1}^{*j})^2 - (\sigma_{x1}^{*j})(\sigma_{y1}^{*j})}\,. \tag{7}$$

In the range j ($j = 1...m$) of the linearized stress-strain curve for the aluminium, the increment of load is:

$$e^j = \frac{\sigma_{e1}^j - \sigma_{e1}^{j-1}}{\sigma_{e1}^{*j}}\,. \tag{8}$$

Finally, with the help of the above load increment (8) each significant point of the load-stress or load-strain characteristic curves for different layers can be determined using *Eq.* ($9.a - c$):

$$\begin{aligned} \sigma_i^j &= \sigma_i^{j-1} + e^j \sigma_i^{*j}\,, \\ \varepsilon_i^j &= \varepsilon_i^{j-1} + e^j \varepsilon_i^{*j}\,, \\ p^j &= p^{j-1} + e^j 1\,, \end{aligned} \tag{9.a - c}$$

where $j = 1...m$; further $\sigma^0 = 0$, $\varepsilon^0 = 0$, $p^0 = 0$.

where $j = 1...m$; further $\sigma^0 = 0$, $\varepsilon^0 = 0$, $p^0 = 0$.

Using the above equations the stress-state analysis of the chosen structure can be carried out to check the chosen cross-sections, by repeating the calculations even the wall thickness just required from the point of strength can be determined. All the results of the calculations presented above are necessary but are not sufficient. In fact there are residual stresses in the structure after the first unloading. These residual stresses have great effect on the acting stresses and service life, too. Therefore the designer must consider these stresses and adjust the optimal value of stiffness and prestressing to get the ideal stress-state. The next chapters deal with these tasks and their solutions.

3. The Optimum Stiffness and Prestressing of Hybrid Structure

It is known that deformation limit of the GRP composite shell is well below that of the aluminium liner. As a result, fracture should always start in the composite shell while the liner is in a state of plastic deformation only. The above conclusion can be accepted in case of single high static load. In case of high cyclic pressure, however, as occurs during refilling and use, fatigue failure starts in the liner. This is why in the chosen construction the fracture always starts in the liner and the damage appears as 'leak before break'. It is reasonable to concentrate on the 'weakest point', the liner and its stress-state which can resist fatigue.

To derive the ideal stress-state in the liner the stress-strain curve in *Fig. 2* is approximated as bilinear and is assumed to be linearly elastic up to R_e with a Young's modulus of E_1^1 and to behave plastic at higher strains with an effective modulus of $E_1^{2^*}$. The changes of working stresses in the liner (σ_{e1}) as a function of internal pressure can now easily be determined and using the calculated values the load characteristics can be built up as shown in *Fig. 4*. The *Fig. 4* represents the changes in working stresses during load cycles at prestressing and at operation. (The load cycle at prestressing consists of test-pressure followed by total unloading while at service the load cycle follows the pressure changes from refilling to complete emptying.) As it can be seen the direction and value of operational stresses generated by the tank refilling and using are determined by the elastic load carrying capacity (p_e) of the liner and the value of prestressing (p_t) in case of prescribed value of filling pressure. Consequently these two parameters should be chosen so that during operation the ideal stress-state shape up, so that after prestressing the residual compression stress let be equal to the allowable stress at compression (σ_{a1}^-) while the value of tensile stress after refilling let be the allowable stress in tension (σ_{a1}^+). Assuming the kinematic

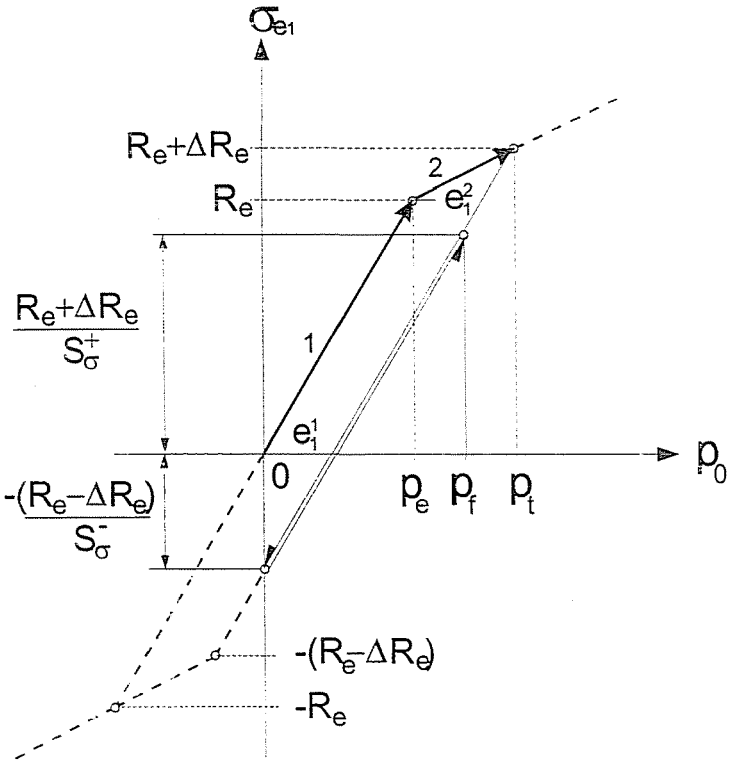

Fig. 4. Linearized stress-pressure diagram of the liner

hardening [3] of the material considering the safety factors for tension S_σ^+ and for compression S_σ^- the allowable stresses can be written as:

$$\sigma_{a1}^+ = \frac{R_e + \Delta R_e}{S_\sigma^+} \quad \text{and} \quad \sigma_{a1}^- = -\frac{R_e - \Delta R_e}{S_\sigma^-} \,. \qquad (10.\ a-b)$$

It is easy to believe that the ideal stress state to resist fatigue is where $S_\sigma^+ = S_\sigma^- = S_\sigma$. From *Fig. 4* this state can be achieved only by optimal pressure ratios of:

$$\left(\frac{p_e}{p_f}\right)_{\text{opt}} = 0.5 S_\sigma \,,$$

$$\left(\frac{p_e}{p_f}\right)_{\text{opt}} = 0.5 S_\sigma (1 + \Delta\overline{R}_e) + 0.5(1 - \Delta\overline{R}_e) \,, \qquad (11.\ a-b)$$

where

$$\Delta\overline{R}_e = \frac{\Delta R_e}{R_e} = \frac{1}{1 + S_\sigma \left(\frac{e_1^1}{e_1^2} - 1\right)} \,. \tag{12}$$

The elastic load carrying capacity of the liner is determined by *Eq.* (11.a) as a special requirement that can be fulfilled by appropriate stiffness of the composite shell. The composite shell has to have an adequate wall thickness to fulfil the strength requirements together with optimal tensile stiffness to achieve the ideal stress-state. Fortunately both above requirements can be fulfilled simultaneously by varying the thickness and winding angle of the wound layers shaping the shell. Regarding the optimal prestressing of the structure it can be carried out after manufacturing and before operation by loading the CNG tank at the optimal pressure calculated from *Eq.* (11.b) followed by depressurization.

4. Designing and Manufacturing of the Optimal CNG Tank

The task is to design and construct a 60 l capacity CNG tank with thin aluminium liner reinforced by glass fibre epoxy which can be built in a vehicle.

The space at disposal can be characterised as length $l_{\max} \leq 950$ mm and diameter $d_{\max} \leq 350$ mm. In order to fulfil the above requirements the liner is made from a tubes with the wall thickness $s_1 = 6.5$ mm and an outer diameter 324 mm. The ends are forged hemispherical heads with varying wall thickness welded to the cylinders as shown in *Fig. 5*. The material for both tube and heads is: AlMgSi1 and the mechanical characteristics of this material (discrete values of the measured stress-strain curve) are given in *Table 1*.

The values given in *Table 1* were measured on specimen manufactured from liner after welding process.

After selecting the liner it will be followed by the designing and manufacturing the glass-epoxy reinforcement so that the hybrid-structure be suitable to withstand safely $p_f = 20$ MPa filling pressure. Wall thickness and winding angle of wound layers in the layered composite shell are in accordance with strength and stiffness requirements and they can be calculated as it was mentioned before. According to strength requirement the allowable stress in direction of fibres at filling pressure is:

$$\sigma_{IIa} \leq \frac{R_{IIB}}{S_{II}} \,, \tag{13}$$

Table 1

j	ε_1^j[%]	σ_{e1}^j[MPa]	E_1^j[MPa]	ν_1^j
1	0.327	226	69010	
2	0.360	240	44207	
3	0.387	248	27037	
4	0.418	255	23548	
5	0.479	262	12046	0.26
6	0.545	267	6587	
7	0.630	271	5070	
8	0.788	278	4632	
9	1.030	282	1526	
10	4.061	306	792	

Fig. 5. The complete aluminium liner

where $R_{IIB} \leq 950$ MPa – the tensile strength in direction of fibres and $S_{II} = 3.65$ – the proposed value of safety factor in case of fully wrapped tanks [4,5].

Taking into consideration all above mentioned facts for $\sigma_{IIa} \leq$ ≤ 260 MPa can be obtained. According to the stiffness requirement given as (11.a) the elastic load carrying capacity is:

$$p_e = 0.5 S_\sigma p_f \tag{14}$$

Table 2

i	d_i[mm]	s_i[mm]	ω_i[°]	E_{xi}[MPa]	E_{yi}[MPa]	ν_{xyi}
2	324.75	0.75	16	46297	13455	0.141
3	326.25	0.75	18	44187	13369	0.159
4	327.75	0.75	22	39471	13212	0.202
5	329.25	0.75	25	35668	13129	0.240
6	332.33	2.33	55	13499	23722	0.703
7	336.99	2.33	60	13142	29346	0.701
8	341.65	2.33	65	13129	35668	0.652
9	346.31	2.33	70	13287	41899	0.566

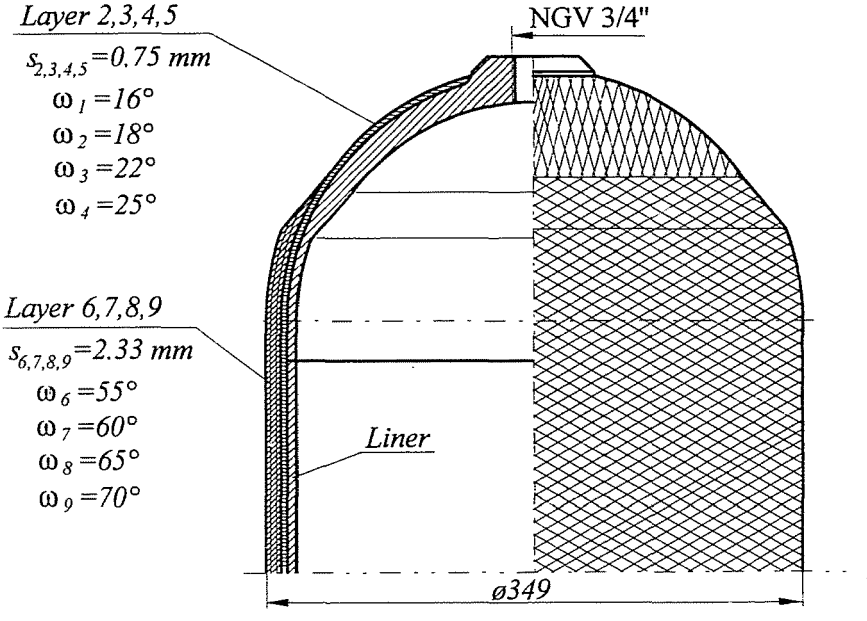

Fig. 6. Sketch of the optimized, fully wrapped 60 l volume CNG tank

from which using at calculation $S_\sigma = 1.25 \times 1.5 \cong 1.9$ for $p_e = 19$ MPa can be gained.

To meet both requirements (9) and (10) the wall thicknesses and winding angles were determined by Computer Aided Design (CAD). The essence of this was the process of optimisation based on the developed analytical method. During the process of optimisation there was a further restriction. The winding angles of layers should be adjusted to the varying

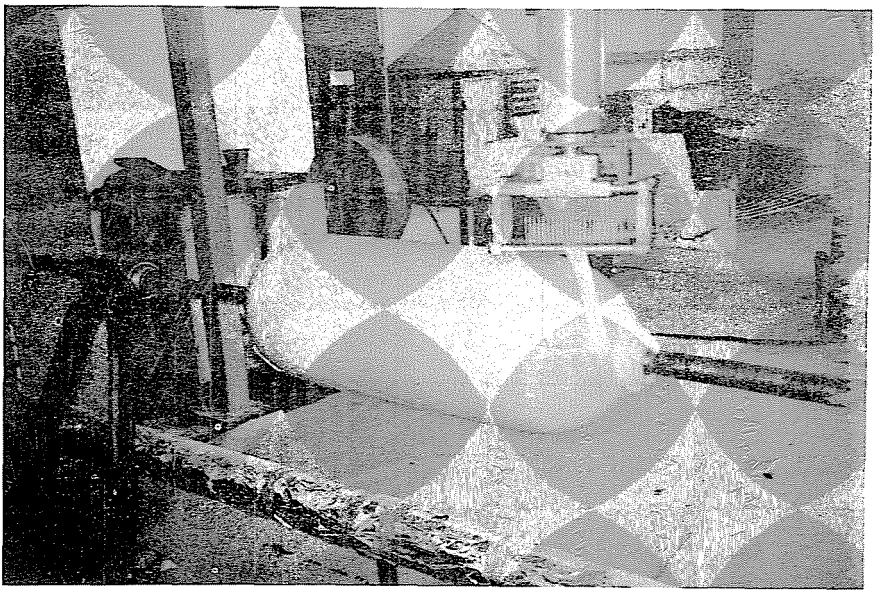

Fig. 7. The automatical winding process

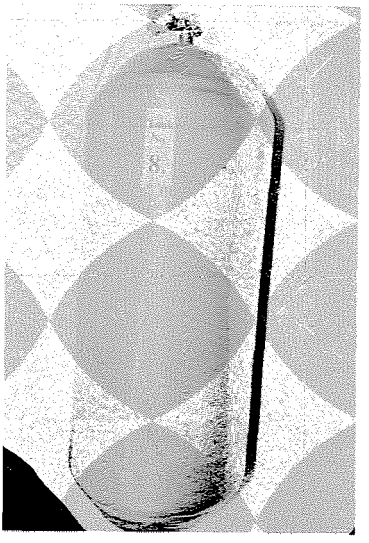

Fig. 8. The prototype of fully wrapped CNG tank

wall thickness of the hemispherical heads to reach the uniform strength as a requirement. The results of this optimisation can be found in *Table 2*

and can bee seen in *Fig. 6*. At the manufacturing of the designed tank the glass-fibre reinforced epoxy layer was prepared by automatic winding process as shown in *Fig. 7*. Finally the mass of the high-pressure gas tank shown in *Fig. 8* was 46 kg which is very near to the required and previously calculated value.

5. Optimal Prestressing of the CNG Tank

The aim of the prestressing is to create ideal residual stress in the liner which causes no fatigue according to Chapter 3. The optimal value of prestressing pressure according to *Eq.* (11.*b*) is:

$$p_t = 0.5 p_f [S_\sigma (1 + \Delta\overline{R}) + 1 - \Delta\overline{R}] \,, \tag{15}$$

where the increment $\Delta\overline{R}$ can be estimated according to the stress-pressure curve of the aluminium liner.

This diagram can be drawn using the previous calculated results and it can be seen in *Fig. 9*. According to this figure the stress-pressure diagram within the investigated range shows good correlation with lines having tangents $e_1^1 = 11.9$ and $e_1^2 \cong 5$ giving $\Delta\overline{R} = 0.276$ using the *Eq.* (12). Taking this fact, the filling pressure and safety factor into consideration for $p_t \cong 31.5$ MPa can be obtained from *Eq.* (15). Following the written method it gives the optimal value of prestressing pressure.

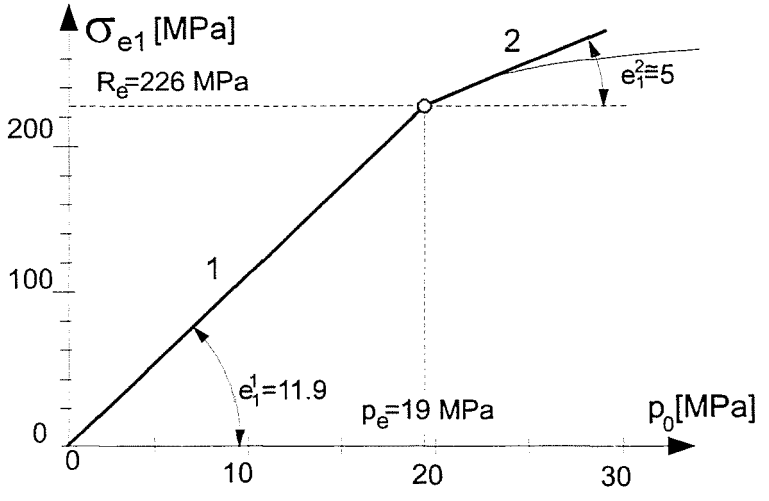

Fig. 9. The stress-pressure characteristic curve of the liner

6. The Stress-State of the CNG Tank

The changes of the stress-state can be followed by using stress-pressure diagram obtained from the calculated results. A typical stress-pressure

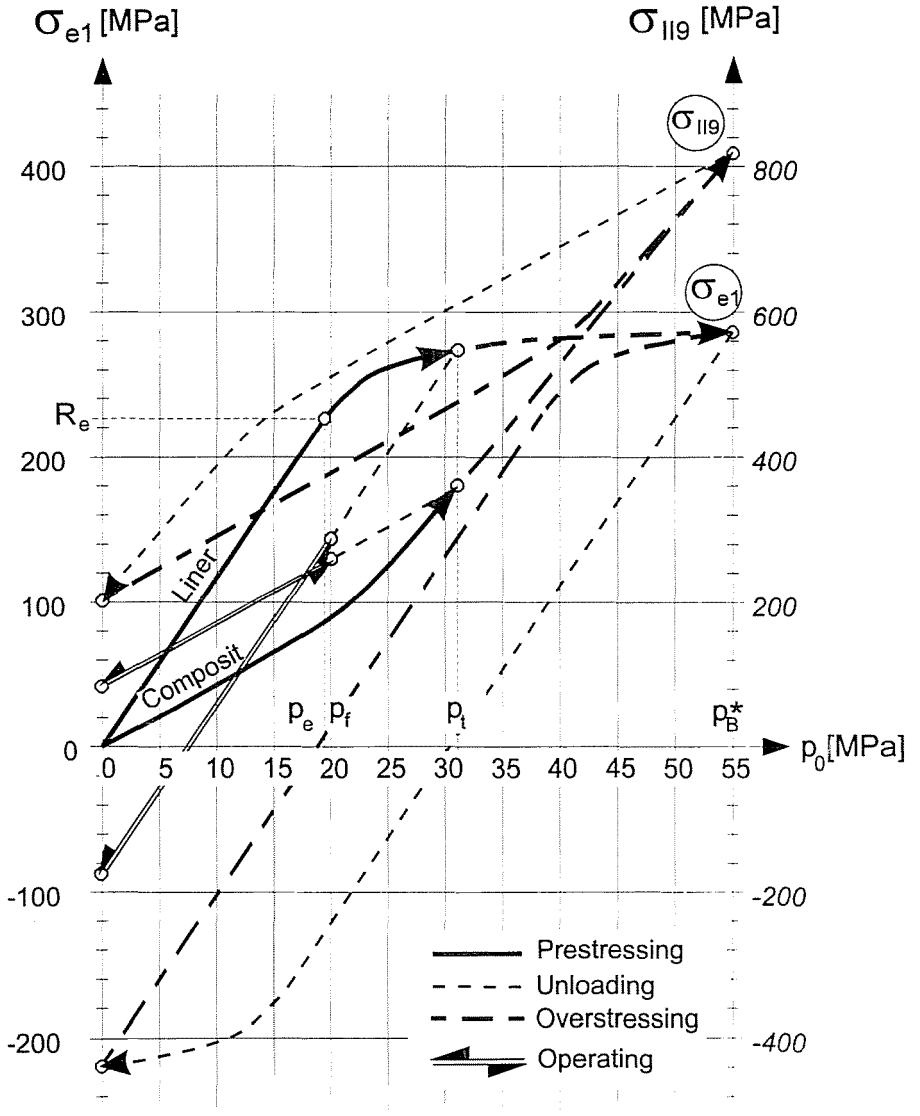

Fig. 10. Stress-pressure diagram of the tank

diagram of the CNG tank can be seen in *Fig. 10*. Besides the optimal prestressing of the tank, *Fig. 10* shows the process of further loading and unloading represents the effect of $p_B^* = 55$ MPa causing low cycle fatigue. Seeing the characteristic values of this figure we can come to the following conclusions:

The highest value of stress acting in the direction of fibres in the composite shell due to the filling pressure is $\sigma_{II9} = 260$ MPa which is just equal to the allowable stress. As a result of the stiffening effect of the composite shell the elastic load carrying capacity of the liner p_e is 19 MPa, just equal to the optimal load carrying capacity of the liner.

After the optimal prestressing of the tank the residual compression stress in the liner is:

$$\sigma_{1e}^- = -92 \text{ MPa} \cong \sigma_{1a}^- = \frac{274 - 2 \times 226}{1.9} = -93.7 \text{ MPa} ,$$

and the tensile stress at filling pressure:

$$\sigma_{1e}^+ = 144 \text{ MPa} \cong \sigma_{1a}^+ = \frac{274}{1.9} = 144 \text{ MPa} .$$

As the stresses calculated are just equal to allowable ones it is clear that during load cycle refilling and draining the ideal stress-state will occur in the liner. The advantageous properties of the structural model are also expected to be valid on the real structure. The aim of the tests is to prove the above mentioned advantageous properties in practice. The results of tests are summed up in the following sections.

7. Tests and Results

There were 2 pcs. of liners and 8 pcs. of full-wrapped tanks tested during this programme. The aim of the tests was to prove the reliability of the suggested method of design; to verify the advantages of the chosen construction; and to complete the construction as a prototype. The tanks tested can be seen on *Fig. 11*.

A summary of the tests is given drawing out the essential conclusions. These are the following:

The tests measured the deformation of CNG tanks under load serving to prove the reliability of calculation model. During these investigations the axial and tangential strains caused by internal pressure were measured by strain-gauges situated on outer surface of the cylindrical body (see *Fig. 12*). The strains measured at different places as a function of internal pressure, are given in *Fig. 13*. The values calculated by numerical method (FEM)

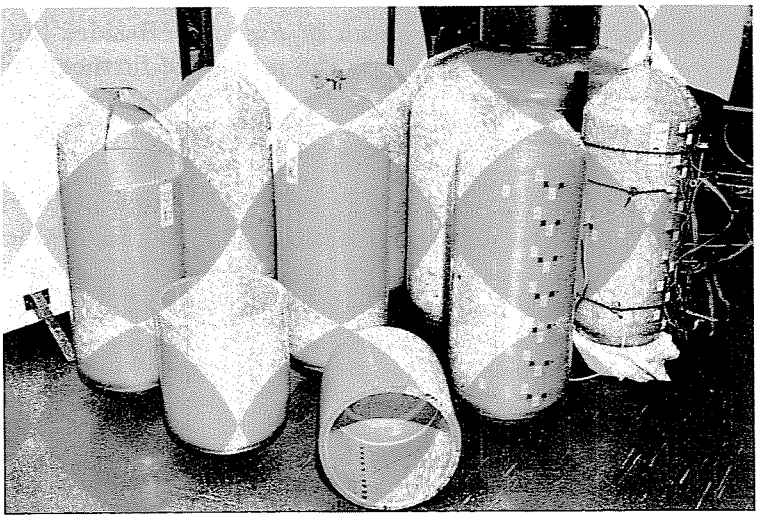

Fig. 11. The group of CNG tank after the tests

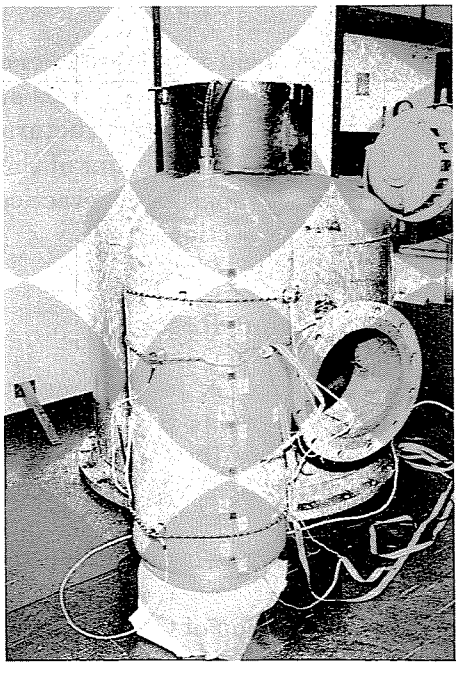

Fig. 12. Strain measurement of the tank

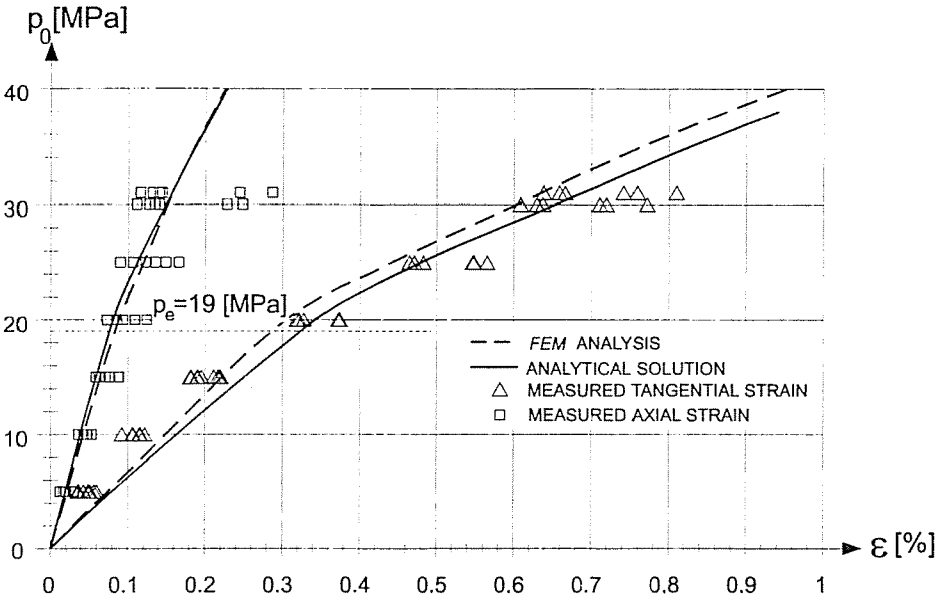

Fig. 13. The strains measured and calculated on the outer surface of the tank

Fig. 14. Leak before break at $p = 560$ bar

and by the simple analytical method are compared. The large deviations arising in strains are not surprising because of the inhomogeneous and

anisotropic engineering material, so they are acceptable. Using this figure the elastic load carrying capacity of the liner can also be predicted or checked, where $p_e \cong 19$ MPa can be regarded a good approximation.

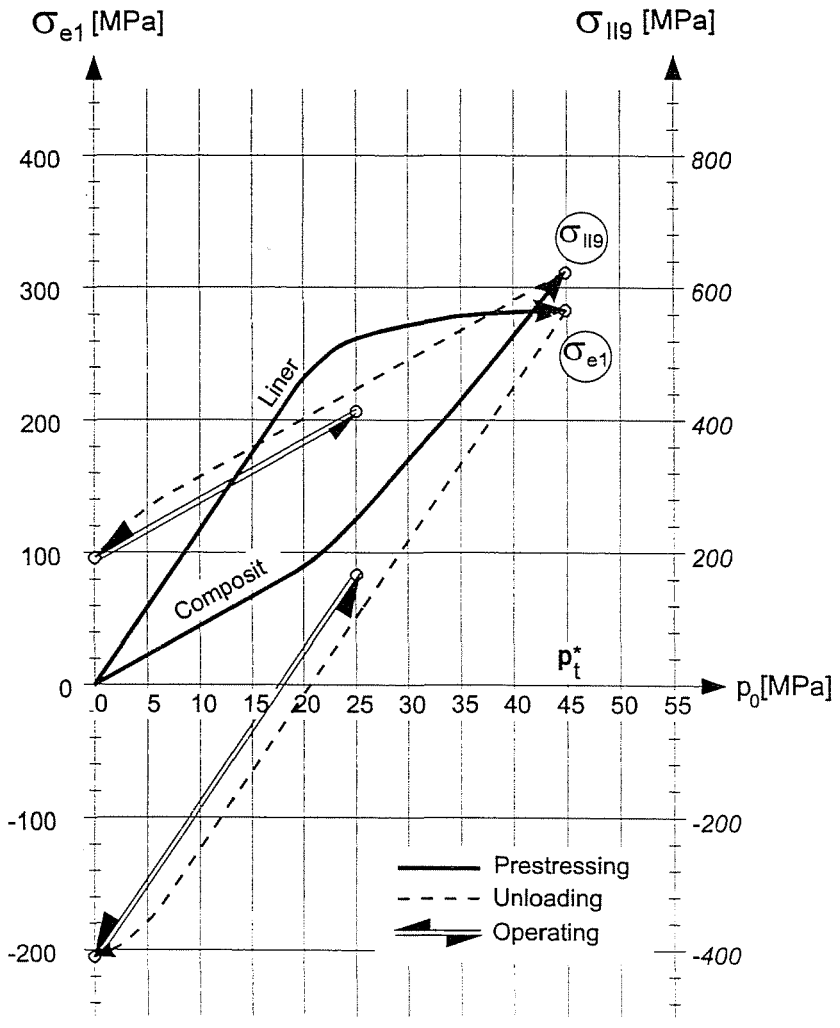

Fig. 15. Stress-pressure diagram of the tank in the case of overstressing

Results of the tests have clearly proved the advantages of optimal prestressing and disadvantages of overstressing and the way of damage. For tubes which had been optimally prestressed (see *Fig. 10*) there were no signs of fatigue up to 8000 load cycles on tank loaded by internal pressure

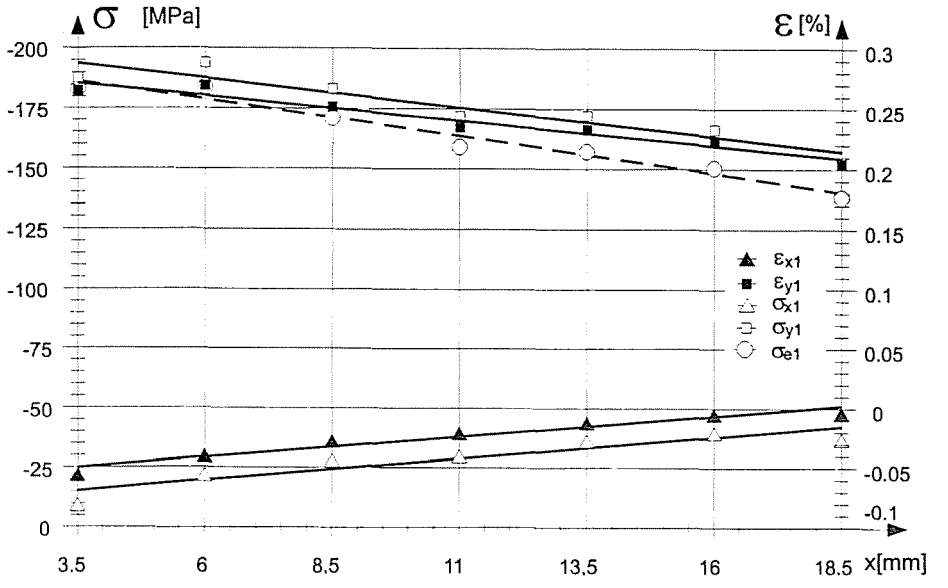

Fig. 16. Residual strains and stresses in the liner

fluctuating $p = 2.5 \div 25$ MPa. The same tank was overloaded with $p_B^* = 55$ MPa followed by fluctuating pressure tests of $p = 0 \div 55$ MPa (causing fatigue) as the characteristic curves on show *Fig. 10*. The investigation on low-cycle fatigue on the tank resulted in 'leak before break' type damage at the welded seam after 5 load cycles as shown in *Fig. 14*.

Useful information was gained from tests on a tank overstressed to $p_t = 45$ MPa internal pressure. In this case the residual stresses in the liner exceed the proportional limit stress as indicated in *Fig. 15*. This is the reason why the liner under $p = 0 \div 25$ MPa fluctuating internal pressure shows leakage before 8000 load cycles. An interesting experience is that leakage regularly stopped on lower pressure ($p < 15$ MPa). Similar phenomena were experienced in further tanks tested. It is very likely, these phenomena can be explained by the existence of residual compressive stresses, which force the cracks to shut. Following fatigue tests the residual stresses and strains in the liner were investigated by use of strain gauges fixed to the internal surface of the sectioned tank. These strain gauges registrated the strains resulting by the cutting of the composite shell. The liner and composite shell are separated from each other due to the elimination of the compressive stresses on sectioning [6]. The values of strains and stresses measured as a function of the distance from the open edge (x) can be seen on *Fig. 16*. The figure, which represents the residual stresses calculated and measured in the vicinity of the open edge, shows good correlation (See *Fig. 15*). It

also can be seen that strains away from open edge, decrease owing to stiffening effect of heads. Further tests and results can be found in report [7].

8. Experiences and Conclusions

During the design, manufacture and test of the new hybrid CNG tank experiences gained result in the following conclusions:

The Computer Aided Design (CAD) based on previously developed analytical and optimisation process can be easily and reliably carried out.

The engineering materials used are cheap and machineable. The aluminium lining with the GRP overwind co-acts excellently giving a high strength and high tensile capacity. The high static load carrying capacity and long service life were the result of the optimal wall thickness and optimal stiffness of the composite shell as well as the optimal prestressing of the tank. Neither corrosion protection nor maintenance at this construction are necessary. Correspondingly the tank can be manufactured relatively cheaply with low specific mass.

Among the special advantages of this new construction is the fact that the damage starts with the fatigue of liner which always appears as 'leak before break'. With this type of damage gas leakage starts at higher pressure but resealing occurs as the pressure drops due to the residual compression stresses originated from prestressing. On the other hand, these stresses after cutting the composite shell will be eliminated by separation of the two components. This means that the old tanks can easily be cut into pieces and the different engineering materials can be recycled separately.

Finally regarding the construction of mass produced tanks, the tests indicate that it will be possible to reduce the aluminium liner wall thickness and allow an improvement in the quality of welded seam and the tube edges can easier be bordered which help to reduce the length of seam. This also gives a reduction of specific mass and manufacturing costs at the tank.

Acknowledgement

The authors wish to express their thanks to European Community for financial subsidizing of this project through the 'Booster Programme'. Also we would like to thank TNO (Netherlands), CISE (Italy) and ANTE (Hungary) for all their outstanding help. Finally we wish to acknowledge the assistance of firms BUDAPLAST, ALUMINIUMÁRUGYÁR and the KOVÁCS RT: for taking part effectively in manufacturing of prototype.

References

1. VARGA, L.: Design of Optimum High-Pressure Monobloc Vessels. *Int. J. Pressure Vessels and Piping.* Vol. 48 (1991) p. 93.
2. CHAWLA, K. K.: Composite Materials. Springer-Verlag Inc. New York, 1987.
3. ZYCKOWSKI, M: Combined Loading in the Theory of Plasticity. PWN-Polish Scientific Publishers, Warszawa, 1981.
4. Proposed American National Standard for Basic Requirements for Compressed Natural Gas Vehicle (NGV) Fuel Containers. AGA NGV2 , 1993.
5. Proposed ISO Standard for High Pressure Cylinders for Natural Gas Vehicles, September, 1992.
6. VARGA, L. – NAGY, A. – KOVÁCS, A: Designing of CNG Tank Made of Aluminium and Reinforced Plastic. *Composites Ref.* No.: 94/17. (in print).
7. Development of a Pressure-proof Lightweight CNG Tank and an Acoustic Emission Based Testing Method for CNG tanks. TNO-report. Report number: 9798/U94.